

## ARTICLE

# Reaction Kinetics of *Trans*-Sobrerol and 8-p-Menthen-1,2-diol with Hydroxyl Radical in Aqueous Solution: A Combined Experimental and Theoretical Study

Yan Long<sup>a</sup>, Xin Tong<sup>a</sup>, Tong-mei Ma<sup>a\*</sup>, Li-ming Wang<sup>a,b\*</sup>

*a.* School of Chemistry & Chemical Engineering, South China University of Technology, Guangzhou 510640, China

*b.* Guangdong Provincial Key Laboratory of Atmospheric Environment and Pollution Control, South China University of Technology, Guangzhou 510006, China

(Dated: Received on April 13, 2015; Accepted on April 27, 2015)

*Trans*-sobrerol (Sob) and 8-p-menthen-1,2-diol (Limo-diol) are the primary products in the atmospheric oxidation of  $\alpha$ -pinene and limonene, respectively. Because of their low volatility, they associate more likely to the liquid particles in the atmosphere, where they are subject to the aqueous phase oxidation by the atmospheric oxidants. In this work, through experimental and theoretical study, we first provide the rate constants of Sob and Limo-diol reacting with hydroxyl radical ( $\cdot\text{OH}$ ) in aqueous solution at room temperature of  $304\pm 3$  K and 1 atm pressure, which are  $(3.05\pm 0.5)\times 10^9$  and  $(4.57\pm 0.2)\times 10^9$  L/(mol·s), respectively. Quantum chemistry calculations have also been employed to demonstrate the solvent effect on the rate constants in aqueous phase and the calculated results agree well with the measurements. Some reaction products have been identified based on liquid chromatography combined with mass spectroscopy and theoretical calculations.

**Key words:** Unsaturated alcohols, Hydroxyl radical, Aqueous-phase reaction, Kinetic, Theoretical calculations

## I. INTRODUCTION

Atmospheric chemical reactions of the volatile organic compounds (VOCs) lead to the formation of second organic aerosols (SOAs) which are the predominant pollutions of the troposphere [1–5], and such a subject has attracted considerable attention and is widely researched recently. Water is considered as the largest component of fine particles (PM<sub>2.5</sub>) globally [6], and provides an important and abundant medium for chemical reactions including formation of SOAs in clouds, fogs and wet aerosols. Some water-soluble organic compounds would dissolve in atmospheric water and undergo aqueous radical reactions to generate considerable SOAs as well [7].

$\alpha$ -Pinene is the second most abundant biogenic non-methane hydrocarbon emitted by vegetation into the atmosphere [8, 9], and is known to contribute to formation of SOAs [10]. *Trans*-sobrerol (Sob) [11] is the significant hydrolysis product of  $\alpha$ -pinene oxide which is an epoxide formed by O atom insertion across the endocyclic double bond in  $\alpha$ -pinene and has been observed as a product in the gas phase photooxida-

tion of  $\alpha$ -pinene in simulation chamber experiments [12, 13]. Limonene is also an important member in the monoterpene family and has high emission rates from both biogenic sources and household solvents [10]. 8-p-Menthen-1,2-diol (Limo-diol) is the main hydrolysis product of limonene oxide, which could be obtained under rather mild conditions [14]. Sob and Limo-diol are water-soluble unsaturated organic alcohols in atmospheric particles.

Several free radicals, such as  $\text{NO}_2$ ,  $\text{O}_3$ ,  $\cdot\text{OH}$ ,  $\text{HO}_2\cdot$ ,  $\text{SO}_4^{\cdot-}$ , and Cl, which can react with dissolved organics, are formed in the atmospheric particulate matters (PM). In these reactions, one of the most efficient and abundant oxidizing species is hydroxyl radical ( $\cdot\text{OH}$ ) [15, 16] which is a reactive electrophile and reacts rapidly and non-selectively with most of the electron-rich sites of organic compounds. The oxidation reactions in PM might enhance the formation of SOAs by producing even less volatile products or reduce the amount of SOA by oxidizing the organic compounds to smaller and therefore more volatile compounds. Therefore, it is necessary to study the reaction kinetics of the low-volatile organic compounds with the atmospheric oxidants in PM, measuring their reaction rate constants, and identifying the reaction products. Researchers have focused more on the reactions of organic compounds with  $\cdot\text{OH}$  in the gaseous phase [7, 17, 18], while there are fewer reports on their reac-

\* Authors to whom correspondence should be addressed. E-mail: tongmei@scut.edu.cn, wanglm@scut.edu.cn

tions in aqueous phase [19–22]. Those aqueous phase reactions that are important to atmospheric chemistry are generally studied by quantum chemical calculations [20, 21] and experimental methods such as gas phase smog chamber, pulse radiolysis, micro-flowtube, laser-photolysis long-path absorption and  $\gamma$ -radiolysis [19]. Herein, we combine experimental rate constant measurements and quantum chemical calculations to elucidate the reaction mechanisms of  $\cdot\text{OH}$  mediated degradation of Sob and Limo-diol in aqueous solution.

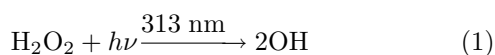
## II. METHODS

### A. Chemicals and reagents

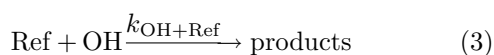
Trans-sobrerol (Sob,  $\geq 97\%$  purity), 4-chlorobenzoic acid (pCBA,  $\geq 98\%$ ), dimethyl phthalate (DMP,  $\geq 99\%$ ) and  $\text{D}_2\text{O}$  were obtained from Shanghai J&K Chemical Reagent (China), and limonene-oxide (Limo-oxide,  $\geq 97\%$ ) were purchased from Sigma-Aldrich (America). Methanol is of high performance liquid chromatography (HPLC) grade while  $\text{H}_2\text{O}_2$  (30%) and all other chemicals are of analytical grade and were used directly without further purification. All solutions were prepared using high purity deionized water from a Milli-Q system. The Limo-diol was synthesized [14] by hydrolyzing limonene-oxide in stirred water solution for 36 h at  $100^\circ\text{C}$  and then transferred to LC-MS for verification. The structures of Sob and Limo-diol are shown in Scheme 1.

### B. Experimental methods

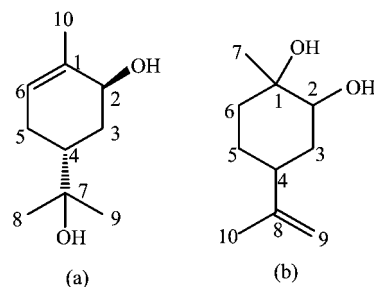
There are a few ways to generate  $\cdot\text{OH}$  in the aqueous phase [19], including UV/ $\text{H}_2\text{O}_2$ ,  $\gamma$ -radiolysis,  $\text{O}_3/\text{H}_2\text{O}_2$ , Fenton method, Walling's method and  $\text{O}_3/\text{OH}$ . In our experiments, UV radiation from ultraviolet mercury lamp ( $\lambda=313\text{ nm}$ ) was used to photolyze  $\text{H}_2\text{O}_2$  to produce  $\cdot\text{OH}$ :



The reaction constants were determined by the relative rate technique [23, 24], in which a reference compound was added to the same solution as the reactant. Both the reactant and the reference compound are subject to reaction with the OH radicals under the same conditions [25]:



The rate constant with the reference compound is well-known already. Samples were taken out of the reactor at different time intervals and the concentrations of the



Scheme 1 Structures of (a) Sob and (b) Limo-diol.

reactant and reference compound were analyzed. The rate constants were then obtained using the following equation:

$$\ln \frac{[\text{alcohol}]_0}{[\text{alcohol}]_t} = \frac{k_{\text{OH-alcohol}}}{k_{\text{OH-Ref}}} \ln \frac{[\text{Ref}]_0}{[\text{Ref}]_t} \quad (4)$$

where  $[\text{alcohol}]_0$ ,  $[\text{alcohol}]_t$ ,  $[\text{Ref}]_0$ , and  $[\text{Ref}]_t$  are the concentrations of reactant and reference compound at time points of 0 and  $t$ , respectively. If the reaction with  $\cdot\text{OH}$  is the only removal mechanism for alcohols and references, a plot of  $\ln([\text{alcohol}]_0/[\text{alcohol}]_t)$  versus  $\ln([\text{Ref}]_0/[\text{Ref}]_t)$  yields a straight line with zero intercept. Multiplying the slope of this linear plot by  $k_{\text{OH+Ref}}$  yields  $k_{\text{OH+alcohol}}$ . The uncertainty of the rate constant, corresponding to the 95% confidence interval and 5% systematic errors, is calculated according to the method similar to Sleiman's [26]:

$$\Delta k = k \sqrt{\left(\frac{\Delta k_{\text{Ref}}}{k_{\text{Ref}}}\right)^2 + \left(\frac{\Delta(\text{slope})}{\text{slope}}\right)^2} \quad (5)$$

Here, p-chlorobenzoic acid (pCBA) [27] and dimethyl phthalate (DMP) were served as reference compounds. One value of  $k_{\text{OH-pCBA}}$  has been previously reported as  $5 \times 10^9\text{ L}/(\text{mol}\cdot\text{s})$  (Michael S, 1999); while there have been four measurements on  $k_{\text{OH-DMP}}$  as:  $(2.67 \pm 0.26) \times 10^9\text{ L}/(\text{mol}\cdot\text{s})$  using the relative rate technique [28],  $4.0 \times 10^9\text{ L}/(\text{mol}\cdot\text{s})$  through fitting the experimental data to the kinetic model [29],  $(3.2 \pm 0.1) \times 10^9$  and  $3.4 \times 10^9\text{ L}/(\text{mol}\cdot\text{s})$  [30] with pulse radiolysis experiments. The experiments were performed in a quartz reactor, which was surrounded by a glass tube with a volume of about 400 mL. Typical initial concentrations were  $10^{-5}$ – $10^{-4}\text{ mol/L}$  for DMP or pCBA, and  $10^{-4}$ – $10^{-3}\text{ mol/L}$  for Limo-diol or Sob. Each of the reactants was mixed with  $\text{H}_2\text{O}_2$  with an initial concentration of 1.0 mmol/L and the solution was stirred under ambient temperature of  $304 \pm 3\text{ K}$  and 1 atm pressure. The solution was then exposed to ultraviolet mercury lamp ( $\gamma=313\text{ nm}$ ) for several minutes. At various intervals, an aliquot of 1 mL sample solutions was transferred to high performance liquid chromatography (HPLC) for analysis.

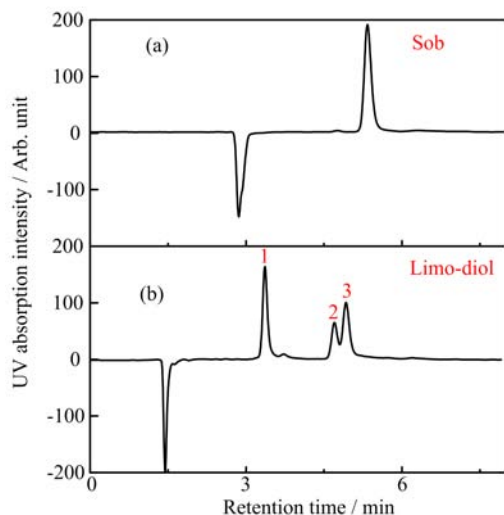


FIG. 1 Detection signals of Sob and Limo-diol with DAD detector at 200 nm from HPLC. 1: Limo-diol-1. 2 and 3: Limo-diol-2.

### C. Analysis

Concentrations of reagents and reference compounds were analyzed by HPLC system, which consists of Agilent 1260, a corresponding diode array detector (DAD) and a reverse phase Ecosil C18 column (250 mm×4.6 mm×5 μm). The working conditions for analysis were as follows. The rate of eluent was 1.0 mL/min and the injected volume was 20 μL for all the samples. The mobile phase contained methanol/water (pH was adjusted to 2 with H<sub>3</sub>PO<sub>4</sub>) with a ratio of 65/35 (volume ratio) for Sob and 55/45 (volume ratio) for Limo-diol. The monitoring wavelength was 200 nm for both Sob and Limo-diol [31], while 235 and 230 nm for pCBA and DMP, respectively. Typical detection signals of Sob and Limo-diol from HPLC are displayed in Fig.1, in which the well-resolved peak signals can be observed. The negative peaks appearing in the figure are solvent peaks. Identification of reaction products was first performed by LC-MS, which consists of Agilent 1290 and maXis impact, and further confirmation was made by comparing the retention time to those having similar chemical constructions and the data based on theoretical calculations.

### D. Computational methods

All calculations were performed with Gaussian 09 programs [32], and M06-2X/6-311++G(2df,2p) were used to optimize the equilibrium geometries and calculate the vibrational frequencies and single point energies. The solvent effect was estimated from single point calculations at M06-2X/6-311++G(2df,2p) level using the polarizable continuum model (PCM) [33] with radii and non-electrostatic terms by SMD model [34]. In sol-

vent effect calculations, the gas-phase M06-2X geometries were used. The Gibbs energy changes in gas phase were corrected to the values in aqueous phase at M06-2X level:

$$\Delta G(\text{aq}) \approx \Delta G(\text{gas}) + \Delta(\Delta G_{\text{sol}}) \quad (6)$$

For the Gibbs barrier heights of bimolecular aqueous reactions, the free energy change converting gas pressure 1 atm to aqueous phase 1 mol/L, 7.9 kJ/mol at 298 K [35], and the solvent cage effect, -10.6 kJ/mol at 298 K [36] were included. The bimolecular rate constants in the aqueous phase are:

$$k_{\text{aq}} = \frac{k_{\text{B}}T}{h} \exp\left(\frac{-\Delta G_{\text{aq}}^{\ddagger}}{RT}\right) \quad (7)$$

where  $k_{\text{B}}$  is the Boltzmann constant,  $h$  is the Planck constant and  $\Delta G_{\text{aq}}^{\ddagger}$  is the standard free energy of activation in aqueous phase.

## III. RESULTS AND DISCUSSION

Many organic compounds exhibit second order hydroxyl radical rate constants of 10<sup>8</sup>–10<sup>10</sup> L/(mol·s) in aqueous phase, which are fairly close to the diffusion controlled limit [22, 37, 38]. The reaction constants of Sob and Limo-diol reacting with ·OH were determined by the relative rate technique, which is described above. In these experiments, to ensure the accuracy of the rate constant, we have selected two different reference compounds as pCBA and DMP, which have different OH rate constants.

### A. Reaction rate constant for Sob+OH

There have been four measurements on the rate constant for the reaction of OH and DMP, obtaining values from (2.67±0.26)×10<sup>9</sup> L/(mol·s) to 4.0×10<sup>9</sup> L/(mol·s), which were all determined at room temperature with pH≥7 [29]. Therefore, we first tried to assess the rate constant of OH+DMP in aqueous phase.  $k_{\text{OH-DMP}}$  was measured by using pCBA as the reference compound with  $k_{\text{OH-pCBA}}$  of 5×10<sup>9</sup> L/(mol·s). The results are shown in Fig.2, from which, the value of  $k_{\text{OH-DMP}}$  is determined as (2.54±0.2)×10<sup>9</sup> L/(mol·s), in agreement with the results obtained using the same method by Xu *et al.* [29]. Therefore, our value of  $k_{\text{OH-DMP}}$  is reasonably suitable to be used as reference standard under the same experimental conditions.

An example of relative kinetic experiments of Sob with ·OH in aqueous phase is shown in Fig.3. The rate constant is obtained as (3.05±0.5)×10<sup>9</sup> L/(mol·s) by averaging the experimental values obtained under different initial concentrations while other reaction conditions unchanged. The kinetic constants of Sob+OH in aqueous solutions with different initial concentrations are given in Table I.

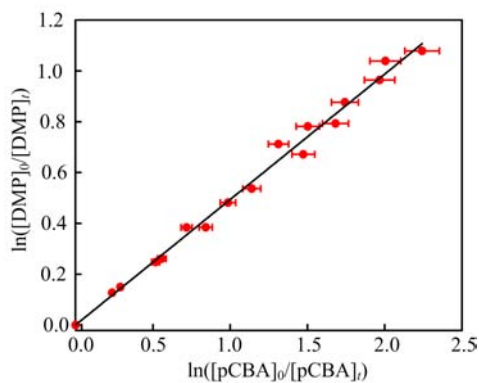


FIG. 2 Relative kinetic rate plot for the reactions of  $\cdot\text{OH}$  with DMP and pCBA in aqueous solution.  $\text{OH}$  was generated from the photolysis of  $\text{H}_2\text{O}_2$  by UV radiation of 313 nm from an ultraviolet mercury lamp.

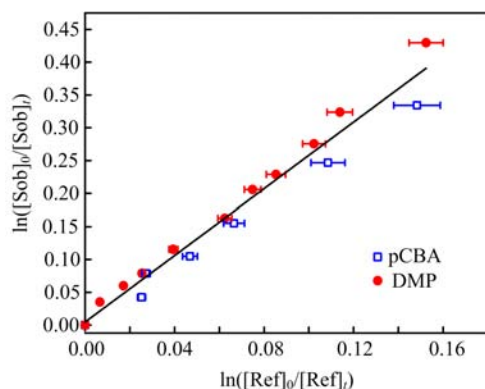


FIG. 3 Relative rate plot for the reaction of  $\cdot\text{OH}$  with Sob in aqueous solution, using pCBA and DMP as reference compounds respectively, the error bar is caused by  $k_{\text{OH-DMP}}$  and the photolysis of pCBA. The rate constant,  $k_{\text{OH-Sob}}$ , is  $(3.05 \pm 0.5) \times 10^9 \text{ L}/(\text{mol}\cdot\text{s})$  when  $[\text{H}_2\text{O}_2]=1.0 \text{ mmol/L}$ ,  $k_{\text{OH-pCBA}}=5 \times 10^9 \text{ L}/(\text{mol}\cdot\text{s})$ ,  $[\text{Ref}]_0 \approx 10 \mu\text{mol/L}$ ,  $[\text{Sob}]_0 \approx 2 \times 10^{-4} \text{ mol/L}$ , and  $k_{\text{OH-DMP}}=(2.54 \pm 0.2) \times 10^9 \text{ L}/(\text{mol}\cdot\text{s})$ .

## B. Hydrolysis products of limonene-oxide

Limo-diol was synthesized by hydrolysis of limonene oxide in  $100^\circ\text{C}$  water solution. After reaction, 1 mmol of a 1:1 mixture of *trans*-(R)-(+)-limonene oxide and *cis*-(R)-(+)-limonene oxide in 12 mL water was stirred for 36 h, the solution was then analyzed by LC-MS. The main hydrolysis product of Limo-diol (yield  $\approx 90\%$ ) [14] was formed as a mixture of four possible conformers (Scheme 2), which might have similar properties. The relative energies have been calculated at M06-2X/6-311+G(d,p) level, conformer d has the lowest energy while the energies of other conformers relative to d are 15.6, 5.1, and 5.4 kJ/mol for a, b and c, respectively. The fractions of the conformers at 298 K are 0.2%, 8.3%, 6.7%, and 84.8%, respectively, when assuming thermal equilibrium among them. The fraction for conformer a is negligible. Their peaks are shown in Fig.1(b)

TABLE I Kinetic constants of Sob+OH in aqueous solutions with different initial concentrations.  $[\text{Sob}]_0$  is in unit of  $10^{-4} \text{ mol/L}$ ,  $[\text{pCBA}]_0$  is in unit of  $10^{-5} \text{ mol/L}$ ,  $[\text{H}_2\text{O}_2]_0=1.0 \text{ mmol/L}$ ,  $k_{\text{OH-Sob}}^*$  in unit of  $10^9 \text{ L}/(\text{mol}\cdot\text{s})$ .

$[\text{Sob}]_0$	$[\text{pCBA}]_0$	$k_{\text{OH-Sob}}^*$	$[\text{Sob}]_0$	$[\text{DMP}]_0$	$k_{\text{OH-Sob}}^*$
1.90	1.02	3.24	2.04	2.01	3.27
3.26	0.98	2.80	2.02	2.03	3.10
1.10	1.13	2.94	2.06	2.06	3.46
4.03	1.20	2.78	1.03	2.02	2.82
0.98	1.09	3.50	2.98	2.00	3.25
2.10	0.95	3.15	3.00	2.21	2.84
			4.10	2.50	3.15

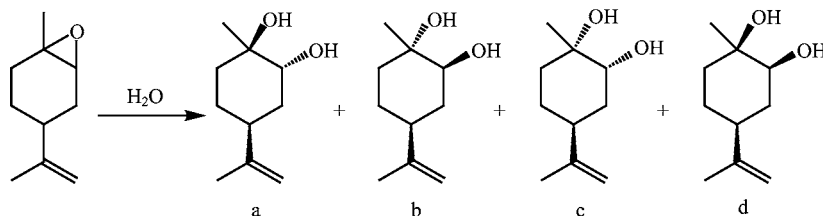
detected by HPLC, the retention time of Limo-diol is 3–6 min, while the counterpart of limonene oxide is approximately 12 min under the same detective condition. Therefore, we assign the first peak in HPLC to conformer d, and the other two peaks to conformers b and c, respectively. Peak 1 has been named as Limo-diol-1, and the peaks 2 and 3 are named as Limo-diol-2 because they could not be separated completely under our detection conditions by HPLC when measuring reaction rates.

The mass spectra of Limo-diol are shown in Fig.4. The mass spectrum in Fig.4(a), which is considered to be conformer d (peak 1 in Fig.1(b)), with  $m/z=211$  (as  $\text{C}_{10}\text{H}_{16}\text{O}-(\text{H}_2\text{O})_2-\text{Na}^+$ , including Na  $m/z=23$  and  $\text{H}_2\text{O}$   $m/z=18$ ), and is more likely to combine with  $\text{H}_2\text{O}$  to generate  $m/z=399$  (as  $2\text{C}_{10}\text{H}_{18}\text{O}_2-(\text{H}_2\text{O})_2-\text{Na}^+$ ) because two hydroxyl radicals are further apart from six-member ring and methyl and its structure is more stable. It has almost the same retention time (about 5 min) as Sob does when tested with the eluent rate of 1.0 mL/min in HPLC. While the mass spectra shown in Fig.4 (b) and (c), with the same  $m/z=193$  (as  $\text{C}_{10}\text{H}_{16}\text{O}-\text{H}_2\text{O}-\text{Na}^+$ , including Na  $m/z=23$  and  $\text{H}_2\text{O}$   $m/z=18$ ) and  $m/z=363$  (as  $2\text{C}_{10}\text{H}_{18}\text{O}_2-\text{Na}^+$ ), are considered to be conformers c and b (peaks of 2 and 3 in Fig.1(b)). As configurational isomers, they have almost the same mass spectrum, and the two peaks always overlapped to each other and could not be separated completely with the reverse-phase C18 column we used, so they were called Limo-diol-2 together.

## C. Reaction rate constant of Limo-diol+OH

The relative kinetic method has been employed to explore the rate constant of the main hydrolysis product, Limo-diol-1, reacting with  $\cdot\text{OH}$  in aqueous phase as mentioned above, pCBA and DMP were used as reference compounds as before. Experimental results are presented in Fig.5. The value of  $k_{\text{OH-Limo-diol-1}}$  has been determined as  $(4.57 \pm 0.2) \times 10^9 \text{ L}/(\text{mol}\cdot\text{s})$  from the slope of the fitting straight line.

With these experiments, the rate constant of



Scheme 2 Structures of Limo-diol, hydrolysis of Limonene-oxide in hot water. These hydrolysis products, including conformers a, b, c, and d, can be detected by HPLC at 200 nm.

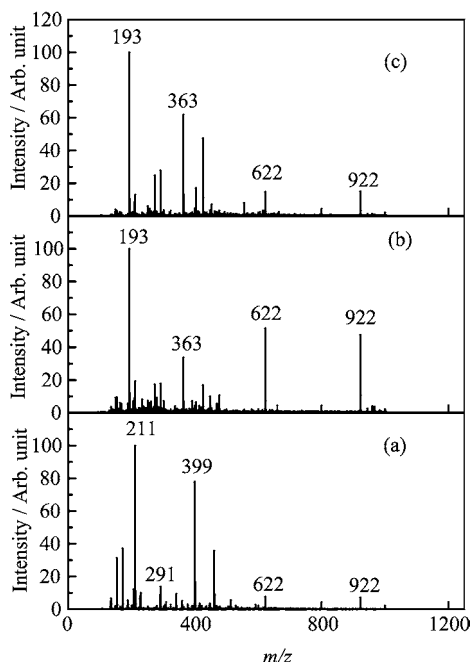


FIG. 4 Mass spectra of Limo-diol, obtained by LC-MS. (a) Limo-diol-1, (b) and (c) Limo-diol-2.

the other hydrolysis product, Limo-diol-2, reacting with OH,  $k_{\text{OH-Limo-diol-2}}$  is determined as  $(2.48 \pm 0.3) \times 10^9 \text{ L}/(\text{mol}\cdot\text{s})$  (Fig.6), and it could be detected with the DAD detector under the same condition as Limo-diol-1 does. We considered peaks 2 and 3 as one compound, Limo-diol-2, because they are isomers and their peaks cannot be separated totally, only one rate constant has been obtained when compared with pCBA. DMP was not used as reference here since its peak was overlapped with Limo-diol-2 when detected by HPLC. Though there is subtle difference between  $k_{\text{OH-Limo-diol-1}}$  and  $k_{\text{OH-Limo-diol-2}}$ ,  $k_{\text{OH-Limo-diol-1}}$  has been considered as  $k_{\text{OH-Limo-diol}}$  because Limo-diol-1 is the main part of Limo-diol and it is likely to be more accurate to use two reference compounds.

For these experiments, the kinetic constants fluctuated in a small range, which may be caused by many factors. Here, we consider that three factors may lead to such a phenomenon. First, the experiments were mainly through manual operation in which there were some

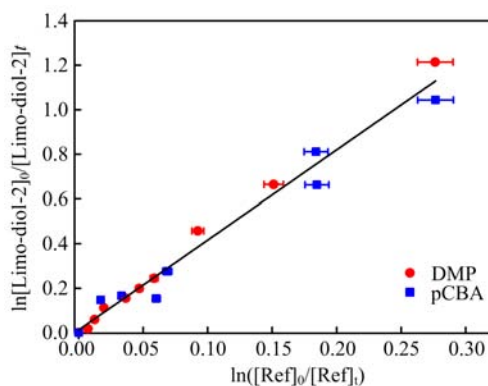


FIG. 5 Relative rate plot for the reaction of  $\cdot\text{OH}$  with Limo-diol-1, using pCBA and DMP as reference compounds, the error bar is caused by  $k_{\text{OH-DMP}}$  and the photolysis of pCBA. The rate constant,  $k_{\text{OH-Limo-diol-1}}$ , is measured as  $(4.57 \pm 0.2) \times 10^9 \text{ L}/(\text{mol}\cdot\text{s})$ , when  $[\text{Limo-diol}]_0 \approx 15 \text{ mmol/L}$ ,  $[\text{Ref}]_0 \approx 20 \text{ }\mu\text{mol/L}$  and  $[\text{H}_2\text{O}_2] = 1.0 \text{ mmol/L}$ .

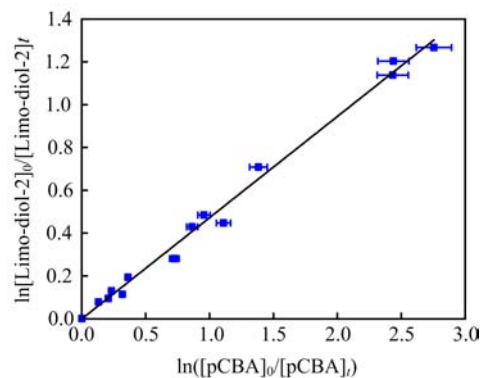


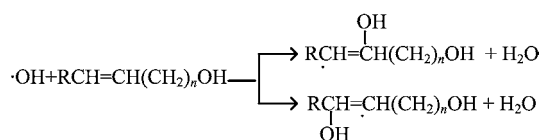
FIG. 6 Example of relative rate plot of hydrolysis products of Limonene oxide, using pCBA as the reference compound under typical concentrations in aqueous solution. The  $k_{\text{OH+Limo-diol-2}}$  was measured to be  $(2.48 \pm 0.3) \times 10^9 \text{ L}/(\text{mol}\cdot\text{s})$ .

uncontrollable conditions compared with laser photolysis method [21]. Moreover, the reference compounds might not be stable during the experimental process, especially for pCBA which can possibly be photolyzed or react with  $\text{H}_2\text{O}_2$  or other reactants (unsaturated alcohols), affecting reaction rate and then resulting in the fluctuation. Furthermore, the reaction temperature [16]

and pH also had small influence on the rate constants. There should be some other factors that may cause the fluctuation of the rate constants and further research is necessary to fully understand the detailed reaction mechanism.

#### D. Reaction kinetic calculations

When considering OH-oxidation reactions of unsaturated organic compounds, there are three possible reaction mechanisms: radical adduct formation (RAF), hydrogen atom transfer (HAT), and single electron transfer (SET), among which, RAF and HAT are the dominant pathways [20]. OH radical can abstract a hydrogen atom from C–H bonds and other bonds, as well as add to unsaturated compounds such as the ones that possess double bonds, *e.g.*, aromatic and heterocyclic ring. The rate constants of addition to unsaturated bonds are often a few times higher than those for H-abstraction from saturated compounds. For the reactions between hydroxyl radical and unsaturated compounds, the branching ratios for H-abstraction are usually small, in the range of 10%–20% [39]. Thus in the case of unsaturated alcohols, the addition reaction would be predominant: With Gaussian 09 programs,



quantum chemical calculations were employed to further explore the reaction rate constants of the two unsaturated alcohols reacting with OH. Here only the major reaction pathway of RAF was considered because other pathways made a small quantity of contribution to the reaction rate and could be neglected. Calculations were carried out at M06-2X/6-311++G(2df,2p) level. The standard free energies of activation in aqueous phase, including unit conversion and solvent cage effect, are 24.2 and 15.4 kJ/mol for OH adding to sites 1 and 6 in Sob, and 23.9 and 13.6 kJ/mol for sites 8 and 9 in Limo-diol (Scheme 1). The barriers for additions of C6 of Sob and C8 of Limo-diol are lower because they have smaller steric hindrance. The rate constants, estimated using the traditional transition state theory, are  $1.28 \times 10^{10}$  and  $2.65 \times 10^{10}$  L/(mol·s) for Sob and Limo-diol, respectively. Though the values are rather reasonable and within the acceptable calculating range [22], there are still minor distinctions between experimental values and calculative ones.

#### IV. CONCLUSION

The kinetic constants for OH reactions with two different unsaturated alcohols, Sob and Limo-diol, which are the primary products in the atmospheric

oxidation of  $\alpha$ -pinene and Limonene, were measured in aqueous phase. Experimental results show that the rate constants are  $(3.05 \pm 0.5) \times 10^9$  and  $(4.57 \pm 0.2) \times 10^9$  L/(mol·s), respectively, under room temperature and neutral condition. The values have been further affirmed with quantum chemistry and kinetics calculations and compared with the values of previous literatures which demonstrated aqueous-phase reactions of OH initiated oxidation of other unsaturated compounds, illustrating our results are quite reasonable. The results obtained in this work give a certain theoretical guidance for VOCs atmospheric liquid reactions.

#### V. ACKNOWLEDGMENTS

This work was supported by the National Natural Science Foundation of China (No.21177041 and No.21107026), the Fundamental Research Funds for the Central Universities (No.2013ZZ0073), and the Scientific Research Foundation for Returned Overseas Chinese Scholars, State Education Ministry.

- [1] P. J. Ziemann, *Int. Rev. Phys. Chem.* **30**, 161 (2011).
- [2] E. U. Emanuelsson, M. Hallquist, K. Kristensen, M. Glasius, B. Bohn, H. Fuchs, B. Kammer, A. Kiendler-Scharr, S. Nehr, F. Rubach, R. Tillmann, A. Wahner, H. C. Wu, and T. F. Mentel, *Atmos. Chem. Phys.* **13**, 2837 (2013).
- [3] J. H. Kroll and J. H. Seinfeld, *Atmos. Environ.* **42**, 3593 (2008).
- [4] V. Varutbangkul, F. J. Brechtel, R. Bahreini, R. Bahreini, N. L. Ng, M. D. Keywood, J. H. Kroll, R. C. Flagan, J. H. Seinfeld, A. Lee, and A. H. Goldstein, *Atmos. Chem. Phys.* **6**, 2367 (2006).
- [5] M. Hallquist, J. C. Wenger, U. Baltensperger, Y. Rudich, D. Simpson, M. Claeys, J. Dommen, N. M. Donahue, C. George, A. H. Goldstein, J. F. Hamilton, H. Herrmann, T. Hoffmann, Y. Iinuma, M. Jang, M. E. Jenkin, J. L. Jimenez, A. Kiendler-Scharr, W. Maenhaut, G. McFiggans, Th. F. Mentel, A. Monod, A. S. H. Prévôt, J. H. Seinfeld, J. D. Surratt, R. Szmigielski, and J. Wildt, *Atmos. Chem. Phys.* **9**, 5155 (2009).
- [6] N. M. Donahue, K. E. H. Hartz, B. Chuong, A. A. Presto, C. O. Stanier, T. Rosenhörn, A. L. Robinson, and S. N. Pandis, *Faraday Discuss.* **130**, 295 (2005).
- [7] J. R. Wells, *Int. J. Chem. Kinet.* **36**, 534 (2004).
- [8] R. J. Griffin, D. R. Cocker, J. H. Seinfeld, and D. Dabdub, *Geophys. Res. Lett.* **26**, 2721 (1999).
- [9] I. G. Kavouras, N. Mihalopoulos, and E. G. Stephanoul, *Nature* **395**, 683 (1998).
- [10] M. Kanakidou, J. H. Seinfeld, S. N. Pandis, I. Barnes, F. J. Dentener, M. C. Facchini, R. Van Dingenen, B. Ervens, A. Nenes, C. J. Nielsen, E. Swietlicki, J. P. Putaud, Y. Balkanski, S. Fuzzi, J. Horth, G. K. Moortgat, R. Winterhalter, C. E. L. Myhre, K. Tsigaridis,

- E. Vignati, E. G. Stephanou, and J. Wilson, *Atmos. Chem. Phys.* **5**, 1053 (2005).
- [11] D. B. Bleier and M. J. Elord, *J. Phys. Chem. A* **117**, 4223 (2013).
- [12] Y. Yu, M. J. Ezell, A. Zelenyuk, D. Imre, L. Alexander, J. Ortega, J. L. Thomas, B. D'Anna, C. W. Harmon, S. N. Johnson, and B. J. Finlayson-Pitts, *Phys. Chem. Chem. Phys.* **10**, 3063 (2008).
- [13] T. Berndt, O. Böge, and F. Stratmann, *Atmos. Environ.* **37**, 3933 (2003).
- [14] Z. Wang, Y. T. Cui, Z. B. Xu, and J. Qu, *J. Org. Chem.* **73**, 2270 (2007).
- [15] H. Hermann, *Chem. Rev.* **103**, 4691 (2003).
- [16] B. Ervens, S. Gligorovski, and H. Herrmann, *Phys. Chem. Chem. Phys.* **5**, 1811 (2003).
- [17] Y. Zhang, K. Chao, J. Sun, Z. Su, X. Pan, J. Zhang, and R. Wang, *J. Phys. Chem. A* **117**, 6629 (2013).
- [18] F. Bernard, I. Magneron, G. Eyglunent, V. Daele, T. J. Wallington, M. D. Hurley, and A. Mellouki, *Environ. Sci. Technol.* **47**, 3182 (2013).
- [19] A. Monod, L. Poulain, S. Grubert, D. Voisin, and H. Wortham, *Atmos. Environ.* **39**, 7667 (2005).
- [20] T. An, Y. Gao, G. Li, P. V. Kamat, J. Peller, and M. V. Joyce, *Environ. Sci. Technol.* **48**, 641 (2014).
- [21] I. Morozov, S. Gligorovski, P. Barzaghi, D. Hoffmann, Y. G. Lazarou, E. Vasiliev, and H. Herrmann, *Int. J. Chem. Kinet.* **40**, 174 (2008).
- [22] G. V. Buxton, C. L. Greenstock, W. P. Helman, A. B. Ross, and W. Tsang, *J. Phys. Chem. Ref. Data* **17**, 513 (1988).
- [23] S. E. Wyatt, I. S. Baxley, and I. R. Wells, *Int. J. Chem. Kinet.* **31**, 551 (1999).
- [24] J. C. Harrison and J. R. Wells, *Atmos. Environ.* **43**, 798 (2009).
- [25] J. R. Wells, *Environ. Sci. Technol.* **39**, 6937 (2005).
- [26] C. Sleiman, G. El Dib, B. Ballesteros, A. Moreno, J. Albaladejo, A. Canosa, and A. Chakir, *J. Phys. Chem. A* **118**, 6163 (2014).
- [27] M. S. Elovitz and U. von Gunten, *Ozone Sci. Eng.* **21**, 239 (1999).
- [28] G. Wen, J. Ma, Z. Q. Liu, and L. Zhao, *J. Hazard. Mater.* **195**, 371 (2011).
- [29] B. Xu, N. Y. Gao, H. Cheng, S. J. Xia, M. Rui, and D. D. Zhao, *J. Hazard. Mater.* **162**, 954 (2009).
- [30] M. H. Wu, N. Liu, G. Xu, J. Ma, L. Tang, L. Wang, and H. Y. Fu, *Radiat. Phys. Chem.* **80**, 420 (2011).
- [31] L. Tao and M. A. Pereira, *J. Chromat. A* **793**, 71 (1998).
- [32] M. J. Frisch, G. W. Trucks, H. B. Schlegel, G. E. Scuseria, M. A. Robb, J. R. Cheeseman, G. Scalmani, V. Barone, B. Mennucci, G. A. Petersson, H. Nakatsuji, M. Caricato, X. Li, H. P. Hratchian, A. F. Izmaylov, J. Bloino, G. Zheng, J. L. Sonnenberg, M. Hada, M. Ehara, K. Toyota, R. Fukuda, J. Hasegawa, M. Ishida, T. Nakajima, Y. Honda, O. Kitao, H. Nakai, T. Vreven, J. A. Jr. Montgomery, J. E. Peralta, F. Ogliaro, M. Bearpark, J. J. Heyd, E. Brothers, K. N. Kudin, V. N. Staroverov, R. Kobayashi, J. Normand, K. Raghavachari, A. Rendell, J. C. Burant, S. S. Iyengar, J. Tomasi, M. Cossi, N. Rega, J. M. Millam, M. Klene, J. E. Knox, J. B. Cross, V. Bakken, C. Adamo, J. Jaramillo, R. Gomperts, R. E. Stratmann, O. Yazyev, A. J. Austin, R. Cammi, C. Pomelli, J. W. Ochterski, R. L. Martin, K. Morokuma, V. G. Zakrzewski, G. A. Voth, P. Salvador, J. J. Dannenberg, S. Dapprich, A. D. Daniels, Ö. Farkas, J. B. Foresman, J. V. Ortiz, J. Cioslowski, and D. J. Fox, *Gaussian 09, Revision A.1.*, Wallingford CT: Gaussian, Inc., (2009).
- [33] G. Scalmani and M. J. Frisch, *J. Chem. Phys.* **132**, 114110 (2010).
- [34] A. V. Marenich, C. J. Cramer, and D. G. Truhlar, *J. Phys. Chem. B* **113**, 6378 (2009).
- [35] M. D. Liptak and G. C. Shields, *J. Am. Chem. Soc.* **123**, 7314 (2001).
- [36] Y. Okuno, *Chem. Eur. J.* **3**, 212 (1997).
- [37] F. J. Benitez, J. Beltran-Heredia, J. L. Acero, and F. J. Rubio, *J. Hazard. Mater. B* **79**, 271 (2000).
- [38] W. R. Haag and C. C. D. Yao, *Environ. Sci. Technol.* **26**, 1005 (1992).
- [39] M. Simic, P. Neta, and E. Hayon, *J. Phys. Chem.* **77**, 2662 (1973).